Received: 15 January 2022 | Revised: 04 March 2022 | Accepted: 06 March 2022
DOI: 10.22034/ecc.2022.324117.1306
Eurasian Chemical Communications
SAMI

FULL PAPER

Preparation and characterization of nano silver nitrate by *Pyrus communis* plant extract (peel and seeds) and biological activity study

Zahraa A. Mahmood* |**Enaam Fadil Mousa** |**Sahar T. Adday**

Department of Chemistry, College of Science for Woman, University of Baghdad, Baghdad, Iraq

***Corresponding Author:**
Zahraa A. Mahmood
Email:
zahraaam_chem@csw.uobaghdad.edu.iq
Tel.: 07821431153

Pyrus communis peel and seeds were used in this study to synthesize silver nanoparticles utilizing a quick and easy method. The plant extract serves as- a reducing and capping agent. To discover the chemicals that cause silver ion reduction, FTIR was used to assess the functional groups in the plant extract. According to a UV-Visible spectrophotometer, the peel had an absorbance peak of 460 nm. In comparison, the seeds had an absorbance peak of 433 nm. The rate of the diameters was discovered using an atomic force microscope to learn about surface topography. The results showed that *Pyrus communis* Peel AgNPs with a diameter of 85.51 nm and *Pyrus communis* seeds with a diameter of 62.50 nm were evaluated for antibacterial and antifungal activity in vitro, and seeds were screened for antibacterial and antifungal activity in vitro. Seeds were shown to be the most inhibitory of the microorganisms tested.

KEYWORDS

AgNPs; Antibacterial; atomic force microscope; UV-Visible.

Introduction

The emergence of multidrug-resistant disease microorganisms has become one of the most pressing issues in medicine worldwide [1]. Nanotechnology developments have laid a solid platform for employing nanoparticles (NPs) to combat disease microorganisms, particularly multidrug-resistant bacteria [2]. Previously, the biocidal characteristics of nanoclusters of numerous metals, primarily silver, gold, zinc, titanium, and bismuth, have been documented [3–5]. Aside from their potential cytotoxicity on human cells, all reactive compounds used in their manufacture may cause cytotoxicity, restricting their usage in clinical practice [6–9]. Chemical reducing agents were used to convert Ag ions into silver nanoparticles (AgNPs) in the classical production of (AgNPs) [10]. Ascorbic acid [11], hydrazine [12], and sodium borohydride [13] are the most often utilized chemical reducing agents. The utilization of these compounds has unintended consequences, and the biocompatibility of the resulting AgNPs makes them unsuitable for application in biological systems when studying their biological efficacy. New green synthesis strategies that utilize environmental chemicals as reducing agents have recently emerged [14–17]. Plants, bacteria, fungi, and algae have all been employed in the green production of metal NPs [18]. A green synthesis approach is used to make AgNPs. AgNPs are being studied for their potential use in biomedicine, such as a bactericide and cancer treatment [19]. For example, Alfalfa Geranium used in the first plants (for the purposes) produces silver nanoparticles with diameters of 2–20 nm and 14–46 nm, respectively [20].

The goal of this study was to make silver nanoparticles from the peel and seeds of Pyrus communis.

Experiment

Preparation of plant extract

In a 250 mL glass beaker, 10 g of Pyrus communis (Peel and Seeds) was mixed with 100 mL distilled water and cooked for 15 min at 80 °C. The extract was allowed to cool to room temperature before filtered through filter paper. Filtrate was collected and kept at 4 °C. The filtrates were employed to reduce and stabilize the pH of the solution [28] (Figure 1).

Preparation of silver nanoparticles

To avoid auto-oxidation of silver, a precise concentration of 0.001 M $AgNO_3$ was prepared by dissolving 0.169 gm $AgNO_3$ in 100 mL distilled water and storing it in a dark glass bottle.

In the single-step green synthesis, 6 mL of (Peel or Seeds) extract were mixed with 10 mL of aqueous $AgNO_3$ solution, stirred for 5 min, and left at room temperature for 24 h before being stored in dark bottles duo to the formation AgNPs [28].

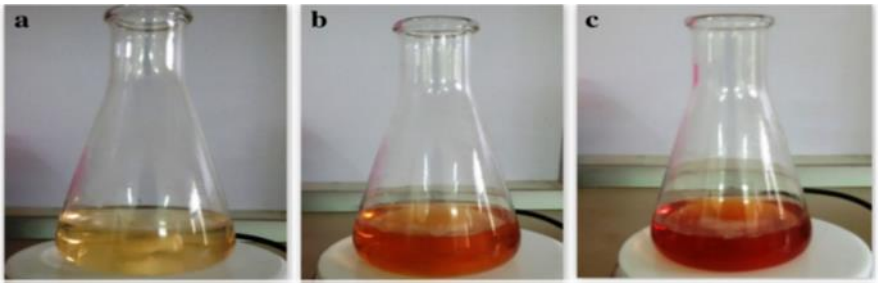

FIGURE 1 color and appearance of *Pyrus communis* seed extract or peel extract (a), synthesized AgNPs using seeds extract (b), and peel extract (c)

Characterization of AgNPs

UV- Visible

Absorption spectroscopy or reflectance spectroscopy in the ultraviolet-visible spectral range is called ultraviolet_visible spectroscopy or ultraviolet-visible spectrophotometer. This means it makes use of visible and neighboring light. The color of the substances involved is directly affected by their absorption or reflectance in the visual spectrum. Atoms and molecules undergo electronic transitions in this region of the electromagnetic spectrum. Absorption spectroscopy is complementary to fluorescence spectroscopy. It measures transitions from the ground to the excited state, whereas fluorescence measures transition from the excited state to the ground state [21].

Fourier transform infrared (FTIR) spectroscopy analysis

FTIR stands for Fourier Transform-Infrared Spectroscopy, and it is a technique for identifying organic (and in certain circumstances inorganic) materials. The absorption bands in the infrared spectrum identify molecular components and structures. An interferometer modulates the wavelength of a broadband infrared source in the FTIR spectrometer. The intensity of transmitted or reflected light has measured a detector as a function of wavelength. The detector's signal is an inter fogram, which must be analyzed using Fourier transforms on a computer to obtain a single-beam infrared spectrum. FTIR spectra are displayed as intensity vs. wave- number (in cm-1) in most cases. The reciprocal of the wavelength is the

wavenumber. At each wavenumber, the intensity can be shown as a percentage of light transmittance or absorption [22].

Atomic force microscopy

Atomic force microscopy (AFM) is a type of scanning probe microscopy (SPM) in which a tiny probe is scanned across the surface of a sample to acquire information about it. The data acquired from the probe's interaction with the surface might range from simple topography to measurements of the material's physical, magnetic, and chemical properties.

At the end of a small cantilever beam, the AFM probe has a very sharp tip, often less than 100 diameter. A piezoelectric scanner tube is linked to the probe, scanning it across a specified sample surface area. As the sample's surface topography (or other qualities) changes, interatomic forces between the probe tip and the sample surface cause the cantilever to deflect. The deflection of the cantilever is measured using laser light reflected from the back of the cantilever. This data is transmitted back to a computer, which creates a topographic map and other relevant attributes. It is possible to photograph areas ranging from roughly 100 nm^2 to less than 100 nm^2 [23].

Results and discussion

UV-Visible absorbance spectroscopy

The silver nanoparticles were characterized using UV-Vis spectroscopy as a preliminary approach. At 24 h, the UV-Vis spectra of the reaction medium were measured to track the decrease of pure Ag+ ions (complete color change). A Shimadzu UV-Vis spectrophotometer, Model 1800, was used to conduct the UV-Vis spectral analysis, which covered the wavelength range of 200 to 1100 nm. The reduction of silver ions in the aqueous solution of nanoparticles might be linked to the UV-Vis spectra of the colloidal solution, which showed substantial absorption at (460 nm for the peel and 433 nm for the seeds) as shown in Figure 2, due to the presence of surface Plasmon resonance silver nanoparticles [24].

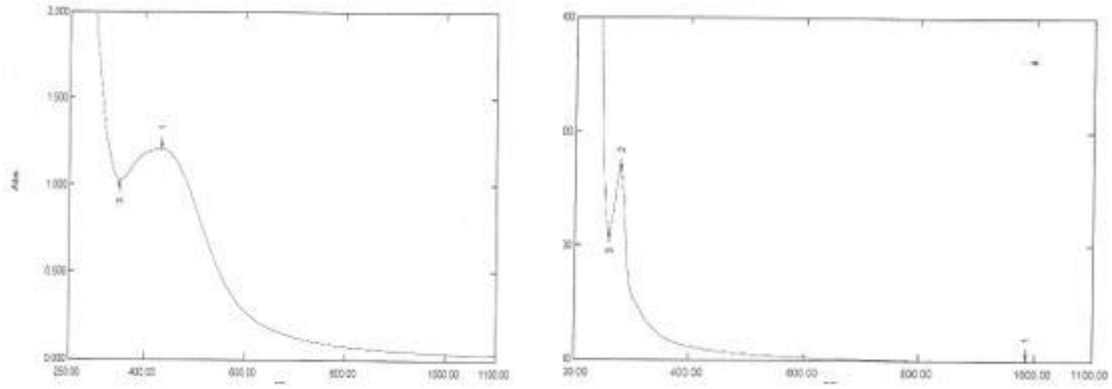

(a) (b)

FIHURE 2 (a) UV -visible spectra of AgNPs from seeds extract, (b) UV-visible spectra of seed extract

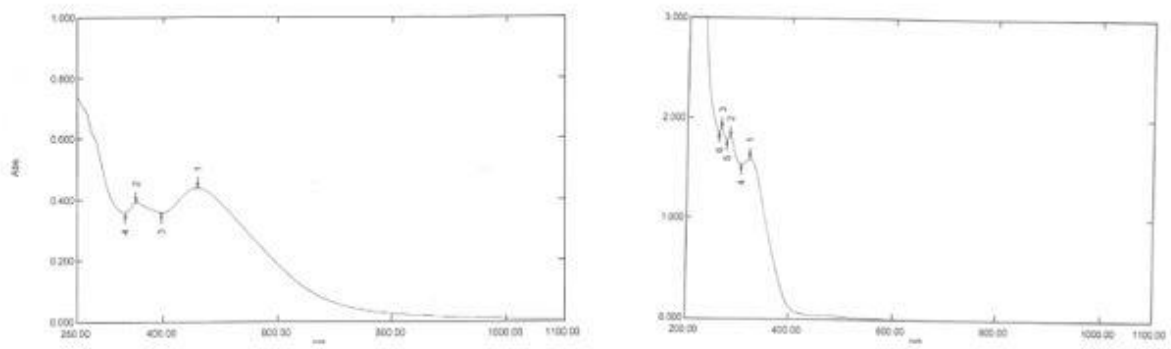

(a) (b)

FIGURE 3 (a) UV-visible spectra of AgNPs from peel extract, (b) UV-visible spectra of peel extract

FTIR analysis

A FTIR investigation was carried out to analyze the functional groups of Pyrus communis Peel and Seeds, and the spectra are presented in Figures 3 and 4. The spectra display a lot of absorption peaks, reflecting their complex character.

Before adding silver nitrate to the seeds, a peak at 3525.88 cm-1 and 3410.15 cm^{-1} was observed due to stretching of the O-H bond of hydroxyl (OH) groups, 3483.44 cm^{-1} was observed due to stretching of the N-H bond of amino groups, and 2927.94 cm-1 and 2854.65 cm^{-1} was observed due to stretching of the C-H bond, as shown in Figure 4-b. After adding silver nitrate to the seeds and forming the nanomaterial, there is a peak at 1068.56 cm^{-1} and 1045.42 cm^{-1} due to the C-O bond bending, 1516.05 cm-1 due to the N-O bond bending, and 1643.35 cm^{-1} due to the C=O bond bending. Figure 5 depicts the spectra (b).

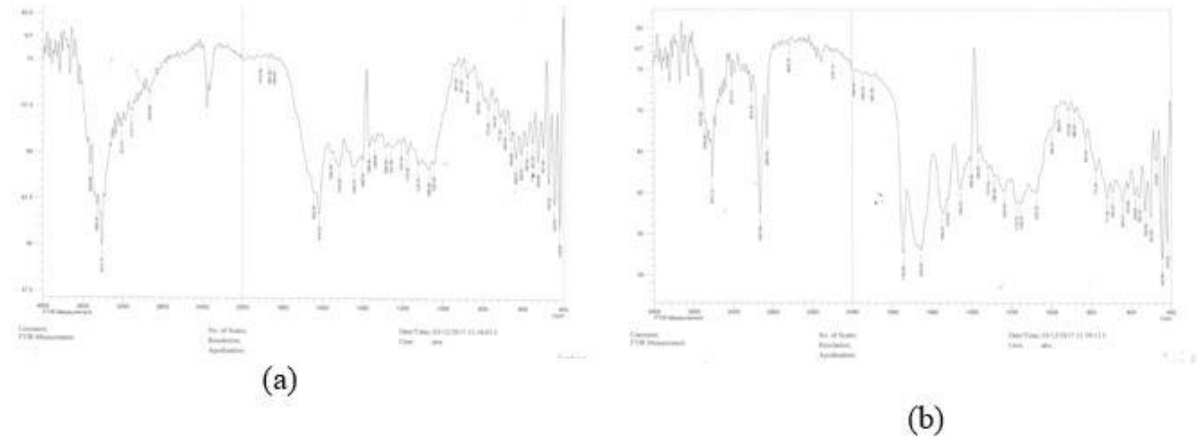

(a) (b)

FIGURE 4 FTIR spectra (a) of Pyrus communis peel extract and (b) of Pyrus communis seeds extract

Apply silver nitrate on the peel first. C-H aliphatic and C-H aromatic bonds are stretching appeared at 2850.79 cm^{-1} and 3047.53 cm^{-1}. respectively, while peaks at 1018.41 cm^{-1}, 1122.57 cm^{-1}, and 1176.58 cm^{-1} attributed to the bending of C=C bond. Also, peaks at 1735.97 cm^{-1} belong to the stretching vibration of C=O bond, while peak at1234.44 cm-1 due to the bending of the C-C bond.

The- stretching- the vibration of bond O-H for (OH) group- appears at 3552.88 cm^{-1} and bending of the C-N bond appears at 1512.19 and 1558.48 cm^{-1} as shown in Figure 4-a.

After that, spray the peel with silver nitrate. The stretching of the N-H bond of the amino group results in a peak at 3479.58 cm^{-1}, as indicated in the spectra in Figure 5-a.

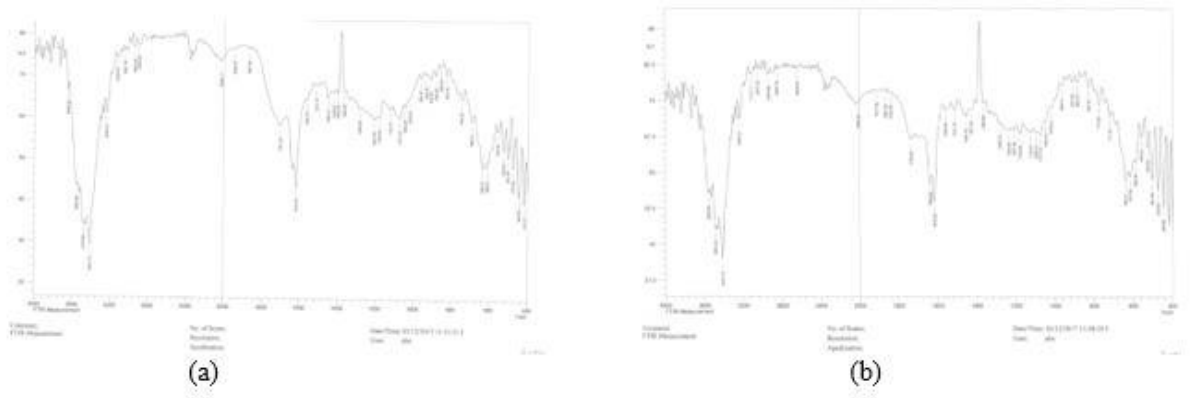

FIGURE 5 FTIR of AgNPs (a) of *Pyrus communis* peel extract and (b) of *Pyrus communis* seeds extract

Atomic force microscopy (AFM)

To learn about surface topography, an atomic force microscope is utilized. It determines the particle diameter rate of the nanoscale size and generates a three-dimensional representation of the material's surface topography. Figure 6 depicts a three-dimensional image of Pyrus communis (a) Peel and (b) Seeds, where the average of diameters was determined (peel 85.51 nm and seeds 62.50 nm).

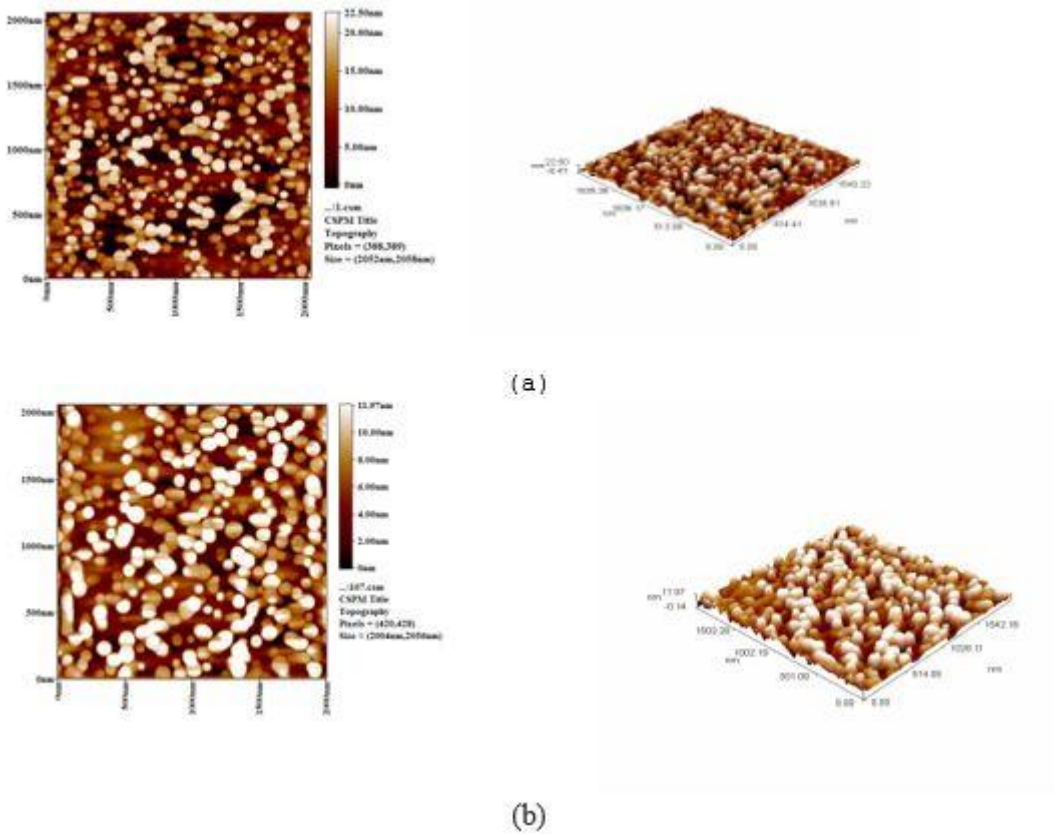

FIGURE 6 AFM images (a) 2D and 3D of AgNPs using *Pyrus communis* seeds extract (b) 2D and 3D of AgNPs using Pyrus communis peel extract

TABLE 1 Average diameters of AgNPs using *Pyrus communis* seeds and peel extract (a) seeds
Avg. Diameter: 62.50 nm

Diameter(nm)<	Volume (%)	Cumulation(%)	Diameter(nm)<	Volume (%)	Cumulation(%)	Diameter(nm)<	Volume (%)	Cumulation(%)
50.00	6.88	6.88	75.00	5.63	83.75	100.00	0.63	98.44
55.00	30.31	37.19	80.00	5.63	89.38	105.00	0.94	99.38
60.00	18.44	55.63	85.00	2.50	91.88	110.00	0.63	100.00
65.00	10.94	66.56	90.00	4.06	95.94			
70.00	11.56	78.13	95.00	1.88	97.81			

(a) Peel
Avg. Diameter: 89.51 nm

Diameter (nm)<	Volume (%)	Cumulation(%)	Diameter (nm)<	Volume (%)	Cumulation(%)	Diameter (nm)<	Volume (%)	Cumulation(%)
85.00	19.23	19.23	95.00	46.15	92.31			
90.00	26.92	46.15	100.00	7.69	100.00			

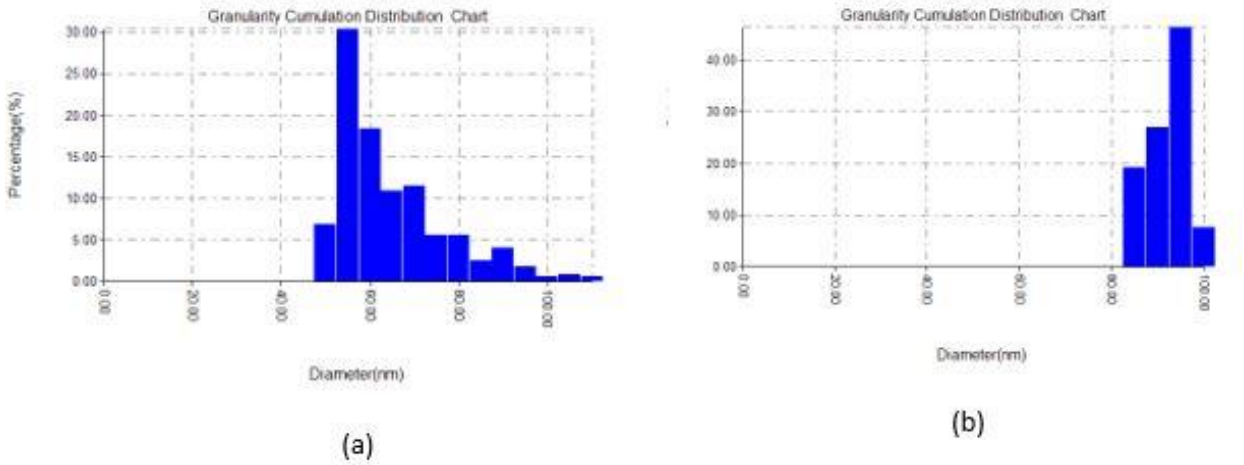

FIGURE 7 Percentage of diameters AgNPs of *Pyrus communis* (a) seeds and (b) peel

Antimicrobial activity

The antibacterial activity of the Peel and Seeds was tested using the disc diffusion technique against gram-positive (Staphylococcus epidermidis and Staphylococcus aureus) and gram-negative bacteria (Pseudomonas aeruginosa and Salmonella SPP) bacteria, as well as fungicidal activity against Candida Albicans [25-27]. For antibacterial activity, Muller Hinton agar was utilized as the culture medium. Table 2 shows the results of a recommended concentration of 25,50,100g/mL of Peel and Seeds in DMSO solvent. Furthermore, the findings regarding microorganism inhibition were compared to positive controls, Amoxicillin medication, and DMSO as a negative control. As shown in Figure 8, peel had a high growth inhibitory effect against Staphylococcus epidermis and Staphylococcus aureus bacteria, and Candida Albicans fungal. In contrast, seeds had no activity against any bacteria except Candida Albicans fungal, which it had good activity against, as demonstrated in Figure 9.

Staphylococcus epitermidis (peel)
Staphylococcus aureus (for peel)
Candida Albicans (for peel)

Figure 8 shows the peel's effectiveness on Staphylococcus epitermidis and Staphylococcus aureus bacteria and, Candida Albicans fungi.

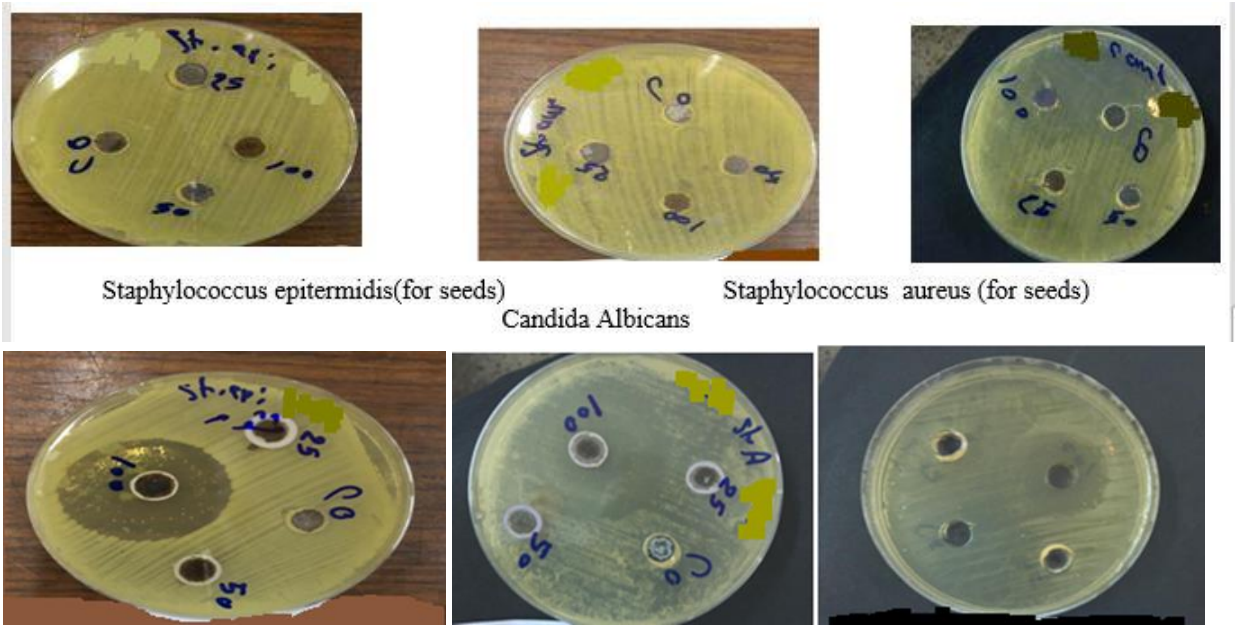

FIGURE 8 shows no inhibition of both Staphylococcus- epitermidis - and Staphylococcus- aureus- bacteria by the seeds, but only inhibition of the Candida Albicans fungi

TABLE 2 Antibacterial and antifungal activities *Pyrus communis* plant extract (peel and seeds)

plant extract	Inhibition Zone Diameter (mm)				
	Staphylococcus epitermidis	Staphylococcus aureus	Pseudomanas aeruginosa	Salmonella SPP	Candida Albicans
Peel	33	40	-	-	21
Seeds	-	-	-	-	29
DMSO	-	-	-	-	-
Amoxicillin	30	38	-	8	24

Conclusion

We described an unprecedented production of silver nanoparticles using Pyrus communis in this publication (Peel and Seeds). Synthesis was shown to be efficient in reaction time and nanoparticle stability when no external stabilizers or reducing agents were used. The peel's absorbance peak was 460 nm, whereas the seeds' absorbance peak was 433 nm, according to a UVeVisible spectrophotometer. Using antibacterial and antifungal testing, Peel exhibited good effectiveness against Gram-positive bacteria and fungal infections (Candida Albicans).

Acknowledgements

The authors acknowledge University of Baghdad, College of Science for Woman for supporting this work.

References

[1] H.M. Lode, R. Stahlmann, M. Kresken, *Zentralbl. Chir.*, **2013**, *138*, 549–553. [crossref], [Google Scholar], [Publisher]
[2] R.Y. Pelgrift, A.J. Friedman, *Adv. Drug Deliv. Rev.*, **2013**, *65*, 1803–1815. [crossref], [Google Scholar], [Publisher]

[3] J.C. Castillo-Martínez, G.A. Martínez-Castañón, F. Martínez-Gutierrez, N.V. Zavala-Alonso, N. Patiño-Marín, N. Niño-Martinez, N.V. Zavala-Alonso, N. Patiño-Marín, C. Cabral-Romero, Journal of Nanomaterials. **2015**, *16*, 177. [crossref], [Google Scholar], [Publisher]
[4] Y.H. Hsueh, W.J. Ke, C.T. Hsieh, K.S. Lin, D.Y. Tzou, C.L. Chiang, *PLoS one*, **2015**, *10*, e0128457. [crossref], [Google Scholar], [Publisher]
[5] N. Nataraj, G.S. Anjusree, A.A. Madhavan, P. Priyanka, D. Sankar, N. Nisha, S.V. Lakshmi, R. Jayakumar, A. Balakrishnan, R. Biswas, *J. Biomed. Nanotechnol.*, **2014**, *10*, 864–870. [crossref], [Google Scholar], [Publisher]
[6] S. Gaillet, J.M. Rouanet, *Food Chem. Toxicol.*, **2015**, *77*, 58–63. [crossref], [Google Scholar], [Publisher]
[7] P.M. Favi, M. Gao, L. Johana Sep´ulveda Arango, S.P. Ospina, M. Morales, J.J. Pavon, T.J. Webster, *J. Biomed. Mater. Res. A.*, **2015**, *103*, 3449–3462. [crossref], [Google Scholar], [Publisher]
[8] M. Czajka, K. Sawicki, K. Sikorska, S. Popek, M. Kruszewski, L. Kapka-Skrzypczak, *Toxicol. In Vitro*, **2015**, *29*, 1042–1052. [crossref], [Google Scholar], [Publisher]
[9] T.H. Chen, C.C. Lin, P.J. Meng, *J. Hazard. Mater.*, **2014**, *277*, 134–140. [crossref], [Google Scholar], [Publisher]
[10] C.A. dos Santos, M.M. Seckler, A.P. Ingle, I. Gupta, S. Galdiero, M. Galdiero, A. Gade, M. Rai, *J. Pharm. Sci.*, **2014**, *103*, 1931–1944. [crossref], [Google Scholar], [Publisher]
[11] S.A. AL-Thabaiti, F.M. Al-Nowaiser, A.Y. Obaid, A.O. Al-Youbi, Z. Khan, *Colloids Surf. B Biointerfaces*, **2008**, *67*, 230–237. [crossref], [Google Scholar], [Publisher]
[12] Z. Khan, S.A. Al-Thabaiti, E.H. El-Mossalamy, A.Y. Obaid, *Colloids Surf. B Biointerfaces*, **2009**, *73*, 284–288. [crossref], [Google Scholar], [Publisher]
[13] L.F. Espinosa-Cristóbal, G.A. Martínez-Castañón, R.E. Martínez-Martínez, J.P. Loyola-Rodríguez, N. Patiño-Marín, J.F. Reyes-Macías, F. Ruiz, *Mater. Lett.,* **2009**, *63*, 2603–2606. [crossref], [Google Scholar], [Publisher]
[14] P. Elia, R. Zach, S. Hazan, S. Kolusheva, Z. Porat, Y. Zeiri, *Int. J. Nanomedicine*, **2014**, *9*, 4007–4021. [crossref], [Google Scholar], [Publisher]
[15] L. David, B. Moldovan, A. Vulcu, L. Olenic, M. Perde-Schrepler, E. Fischer-Fodor, A. Florea, M. Crisan, I. Chiorean, S. Clichici, G.A. Filip, *Colloids Surf. B: Biointerfaces*, **2014**, *122*, 767–777. [crossref], [Google Scholar], [Publisher]
[16] K. Veerakumar, M. Govindarajan, *Parasitol. Res.*, **2014**, *113*, 4085–4096. [crossref], [Google Scholar], [Publisher]
[17] A. Kalaiselvi, S.M. Roopan, G. Madhumitha, C. Ramalingam, G. Elango, *Spectrochim. Acta A Mol. Biomol. Spectrosc.*, **2015,** *135*, 116–119. [crossref], [Google Scholar], [Publisher]
[18] A. El-Faham, A.A. Elzatahry, Z.A. Al-Othman, E.A. Elsayed, *Int. J. Nanomedicine*, **2014**, *9*, 1167–1174. [crossref], [Google Scholar], [Publisher]
[19] P. Rauwel, S. Küünal, S. Ferdov, E. Rauwel, *Adv. Mater. Sci. Eng.*, **2015**, *2015*, Article ID 682749. [crossref], [Google Scholar], [Publisher]
[20] J.L. Gardea-Torresdey, E. Gomez, J.R. Peralta-Videa, J.G. Parsons, H. Troiani, M. Jose-Yacaman, *Langmuir*, **2003**, *19*, 1357–1361. [crossref], [Google Scholar], [Publisher]
[21] Langmuir, 2003. vol. 19. no. 4. pp. 1357–136 [crossref], [Google Scholar], [Publisher]
[22] D.A. Skoog, F.J. Holler, S.R. Crouch, Principles of Instrumental Analysis (6th ed.). Belmont, CA: Thomson Brooks/Cole, **2007**, 169–173. [Google Scholar], [Publisher]
[23] P.R. Griffiths, J.A. de Hasseth, Wiley-Blackwell, **2007**. [Google Scholar], [Publisher]
[24] F.J. Giessibl, *Rev. Mod. Phys.*, **2003**, *75*, 949–983. [crossref], [Google Scholar], [Publisher]
[25] M.J. Firdhouse, P. Lalitha, S.K. Sripathi, *Der Pharma Chem.*, **2012**, *4*, 2320-2326. [Google Scholar], [Publisher]
[26] W.F. Oliveira, *J. Hosp. Infect.*, **2018**, *98*, 111-117. [crossref], [Google Scholar], [Publisher]

[27] E.O. Al-Tamimi, E.F. Mousa, *Baghdad Sci. J.*, **2017**, *14*, 756-764. [crossref], [Google Scholar], [Publisher]
[28] E.F. Mousa, S.H. Merza, *Ann. Rom. Soc. Cell. Biol.*, **2021**, *25*, 5087–5102. [Google Scholar], [Publisher]
[29] V. Parashar, R. Parashar, B. Sharma, A.C. Pandey, *J. Nanomater. Biostructures*. **2009**, *4*, 45-50. [Google Scholar], [Publisher]

How to cite this article: Zahraa A. Mahmood*, Enaam Fadil Mousa, Sahar T. Adday. Preparation and characterization of nano silver nitrate by *Pyrus communis* plant extract (peel and seeds) and biological activity study. *Eurasian Chemical Communications*, 2022, 4(8), 732-740. **Link:** http://www.echemcom.com/article_147683.html